



An *Ab Initio* Study of Some Free-Radical Homolytic Substitution Reactions at Halogen

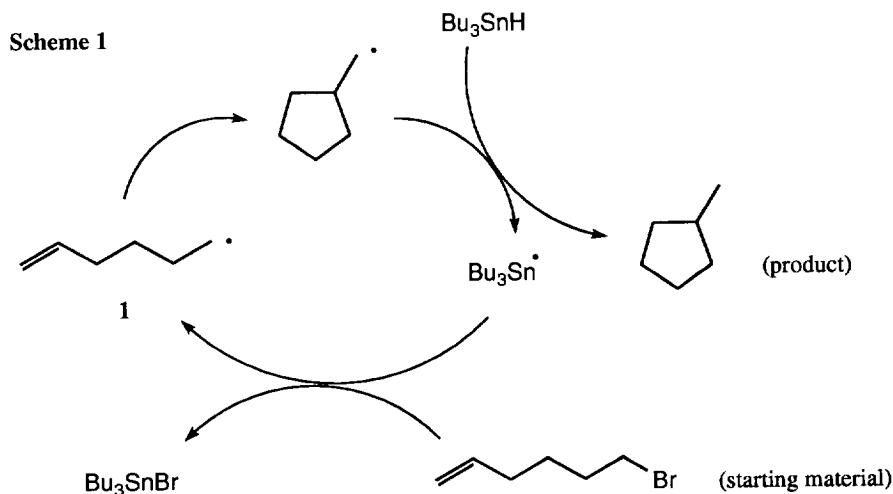
Carl H. Schiesser*, Bruce A. Smart and Tu-Anh Tran

School of Chemistry, The University of Melbourne, Parkville, Victoria, Australia, 3052

Abstract: *Ab initio molecular orbital calculations using pseudopotential basis sets and electron correlation (MP2, QCISD) predict that homolytic substitution by hydrogen atom as well as methyl, silyl, germyl and stannyl radicals at the chlorine, bromine and iodine atoms in hydrogen halides and halomethanes proceeds smoothly and without the formation of hypervalent (9-X-3) intermediates.*

Introduction

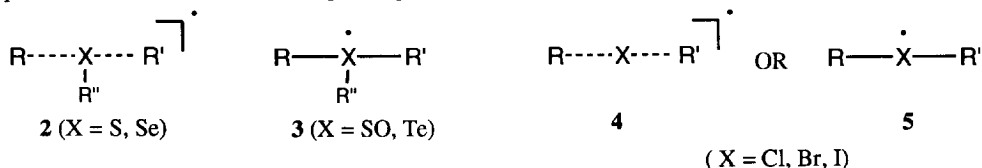
Free-radical chemistry offers the synthetic chemist elegant, efficient and convenient methods for the preparation of a wide range of organic molecules of biological and other significance.¹ This has largely come about as the result of our increased understanding of free-radical processes through important contributions by Julia², Ingold,^{3,4} Beckwith^{4,5} and others⁶ over the past three decades and the ready availability of new precursors and reagents designed specifically for radical-based syntheses.⁷



Many free-radical sequences involve the use of homolytic addition by carbon-centred radicals to an unsaturated moiety as the key step in the overall strategy, as illustrated in Scheme 1 for the homolytic cyclization of the 5-hexenyl radical (1). These radicals, in turn, are often generated by intermolecular homolytic substitution of tin, germanium or silicon-centred chain carrying radicals at the chlorine, bromine or iodine atom in alkyl halides.^{1,8-14} Despite the homolytic substitution reaction being of importance in these sequences, the

intimate mechanistic details of the radical attack at halogen are still ambiguous.

Recently, work in our laboratories has been directed toward the understanding and utilization of free-radical homolytic substitution chemistry at sulfur, selenium and tellurium. We reported for the first time that high-level *ab initio* molecular orbital calculations, using both all-electron and pseudopotential basis sets, predict free-radical attack of hydrogen atom at the sulfur atom in hydrogen sulfide, the selenium atom in hydrogen selenide and the tellurium atom in hydrogen telluride to proceed via T-shaped hypervalent (9-X-3) intermediates.¹⁵ Similar calculations suggest that attack of alkyl radical at the chalcogen in alkyl sulfides^{16,17} and selenides^{16,17} proceeds via T-shaped transition states (2), while attack at the sulfur atom in alkyl sulfoxides¹⁶ and the tellurium atom in alkyl tellurides¹⁹ involve hypervalent intermediates (3) which undergo subsequent dissociation to afford the expected products.



There is experimental evidence to suggest that similar homolytic substitution processes at the bromine atom in alkyl bromides involve smooth transition states (4) while the analogous reaction at iodine is speculated to involve hypervalent (9-I-3) intermediates (5) on the basis of relative rate data.^{20,21}

In order to provide insight into the intimate details of the mechanism of homolytic substitution at halogen, we undertook an extensive high-level *ab initio* study using pseudopotential basis sets, the details of which we now present.

Methods

Previous work had already established the superiority of the pseudopotential basis set of Hay and Wadt for calculating the nature of the stationary points involved in free-radical attack at chalcogen.¹⁵ In this work, all *ab initio* molecular orbital calculations were carried out using the Gaussian 92 program.²² Geometry optimisations and vibrational frequencies were performed using standard gradient techniques at the SCF, MP2 and QCISD levels of theory where possible using RHF and UHF methods for closed and open shell systems, respectively.²³ When correlated methods were used calculations were performed using the frozen core approximation.

All vibrational frequencies were calculated numerically from analytic first derivatives to determine the nature of all located stationary points. Calculations were performed on all reactants, products and transition states to obtain barriers and energies of reaction.

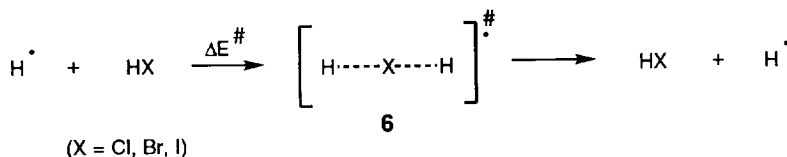
The double- ζ pseudopotential basis sets of Hay and Wadt²⁴⁻²⁶ supplemented with a single set of d-type polarisation functions (exponents as recommended by Höllwarth and co-workers²⁷) were used for Cl, Br, I, Si, Ge and Sn while the double- ζ all-electron basis sets of Dunning²⁸ with an additional set of polarisation functions (exponents $d(\zeta)_C = 0.75$ and $p(\zeta)_H = 1.00$) were used for C and H.

Results and Discussion

Reaction of Hydrogen Atom with Hydrogen Halides

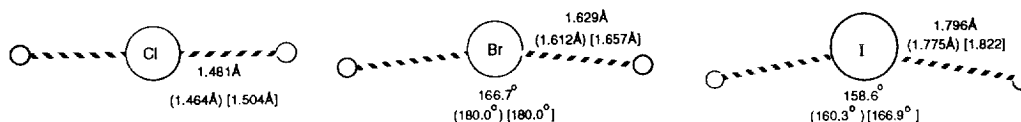
We first turned our attention to the homolytic attack of hydrogen atom at the halogen in hydrogen chloride, bromide and iodide (Scheme 2). Interestingly, the λ^3 -halogenyl species (**6**) were found to correspond to transition states at all levels of theory. At the SCF level, these transition states are predicted to be linear, with halogen - hydrogen distances of 1.504Å, 1.657Å and 1.822Å for the chlorine-, bromine- and iodine-containing species respectively.

Scheme 2



Inclusion of electron correlation has only a small effect on the transition state distances, however, the iodanyl structure (**6**: X = I) is predicted to deviate from linearity when MP2 correlation is included, with a calculated H-I-H angle of 160.3°, while both the brominyl (**6**: X = Br) and iodanyl (**6**: X = I) species are predicted to be non-linear when QCISD is included in the optimization, the former is predicted to have an H-Br-H angle of 166.7°, while the similar angle in the latter is predicted to be 158.6° (Figure 1).

Figure 1. QCISD Calculated Geometries^a of the Transition States (**6**) involved in the Homolytic Substitution of Hydrogen Atom at the Halogen in Hydrogen Chloride, Bromide and Iodide (MP2 Data in Parentheses) [SCF Data in Square Parentheses].



^aFor description of basis set used, see text.

It is useful to compare these data with previous calculations performed in our laboratories. Hypervalent structures involved in the homolytic substitution of hydrogen atom at the selenium atom in hydrogen selenide, the sulfur atom in hydrogen sulfide and the tellurium atom in hydrogen telluride are also predicted to deviate from the anticipated T-shaped geometry.^{15,16,18} This deviation has been explained in terms of hyperconjugative stabilization of those species containing hydrogen in the apical position of the (hypothetical) trigonal bipyramid due to overlap between the lone-pairs of electrons on the central heteroatom and the hydrogen s-orbital.¹⁸

Table 1. SCF, MP2 and QCISD Calculated Energies of the Transition States^a (**6**) (E) and Energy Barriers^b (ΔE^\ddagger) for the Homolytic Substitution of Hydrogen Atom at the Halogen in Hydrogen Chloride, Bromide and Iodide.

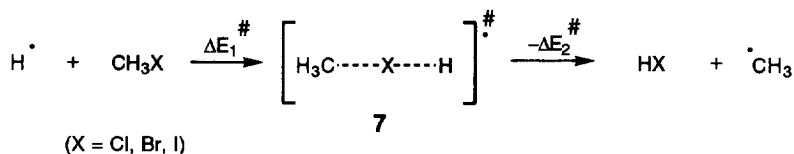
Transition State (6)	SCF		MP2		QCISD	
	E	ΔE^\ddagger	E	ΔE^\ddagger	E	ΔE^\ddagger
H ₂ Cl	-15.75040	139.5	-15.89818	122.4	-15.91921	104.8
H ₂ Br	-13.98021	101.9	-14.10965	90.3	-14.13044	74.3
H ₂ I	-12.21225	74.3	-12.32610	64.4	-12.34655	47.2

^aEnergies in Hartrees (1H = 2625.5 kJ.mol⁻¹). For details of the basis set used, see text. ^bEnergies in kJ.mol⁻¹.

Table 1 lists the calculated activation energies (ΔE^\ddagger) for the reactions depicted in Scheme 2 along with the calculated energies (E) of the transition states (**6**). Inspection of Table 1 reveals that, as expected, attack at iodine is most favourable, with calculated barriers of 74.3, 64.4 and 47.2 kJ.mol⁻¹ at the SCF, MP2 and QCISD levels of theory respectively, while attack at bromine and chlorine is somewhat less favourable (ΔE^\ddagger = 74.3 kJ.mol⁻¹ (Br, QCISD); 104.8 kJ.mol⁻¹ (Cl, QCISD)).

Reaction of Hydrogen Atom with Halomethanes

Scheme 3

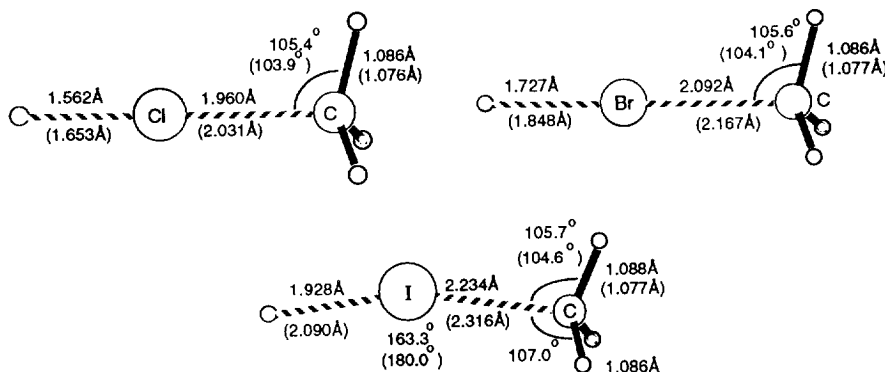


The hypervalent methyl- λ^3 -halogenyl species (**7**), namely methyl- λ^3 -chlorinyl (MeClH), methyl- λ^3 -brominyl (MeBrH) and methyl- λ^3 -iodinyl (MeIH) were located on their respective potential energy surfaces and proved to correspond to transition states at both SCF and MP2 levels of theory. As was observed for the smaller analogues (**6**), at SCF level the C-X-H angle is predicted to be linear, while at the MP2 level methyl- λ^3 -iodinyl is predicted to deviate from linearity, with a C-I-H angle of 163.3°. Calculated geometries are displayed in Figure 2, while the energy barriers (ΔE_1^\ddagger , ΔE_2^\ddagger) for the forward and reverse reactions as depicted in Scheme 3 are listed in Table 2. Calculated energies of the transition states (**7**) are listed in Table 5 along with other structures in this study.

Inspection of the data in Table 2 and Figure 2 reveals that hydrogen atom is a better attacking radical than methyl and that methyl radical is the better leaving group. This manifests itself as *earlier* transition states to those observed for the attack of hydrogen atom at the hydrogen halides and lower barriers for the forward reaction as compared to the reverse. For example, structure (**7**, X = I) has an H-I separation of 1.928 Å (MP2) as compared with 1.776 Å in **6** (X = I) at the same level of theory. In addition, QCISD/MP2 single-point calculations predict energy barriers of only 72.7, 44.0 and 23.4 kJ.mol⁻¹ for the substitution of hydrogen atom at the chlorine, bromine and iodine atom with expulsion of methyl radical, while the reverse reactions have

considerably higher barriers at 162.5, 125.4 and 97.9 kJ.mol⁻¹ at the same level of theory. Similar conclusions were reached in studies of homolytic substitution at the selenium atom in alkyl selenides.¹⁸

Figure 2. MP2 Calculated Geometries^a of the Transition States (7) involved in the Homolytic Substitution of Hydrogen Atom at the Halogen in Chloromethane, Bromomethane and Iodomethane (MP2 Data in Parentheses).



^aFor description of basis set used, see text.

Table 2. SCF, MP2 and QCISD/MP2 Calculated Energy Barriers^a (ΔE_1^\ddagger , ΔE_2^\ddagger) for the Forward and Reverse Homolytic Substitution Reactions of Hydrogen Atom at the Halogen Atom in Chloromethane, Bromomethane and Iodomethane (Scheme 4).

Transition State (7)	SCF		MP2		QCISD/MP2	
	ΔE_1^\ddagger	ΔE_2^\ddagger	ΔE_1^\ddagger	ΔE_2^\ddagger	ΔE_1^\ddagger	ΔE_2^\ddagger
CH ₃ ClH	97.5	197.6	92.5	164.5	72.7	162.5
CH ₃ BrH	62.4	155.4	65.5	124.0	44.0	125.4
CH ₃ IH	38.3	125.3	45.6	95.2	23.4	97.9

^aEnergies in kJ.mol⁻¹. For details of the basis set used, see text.

These calculations suggest that homolytic substitution of hydrogen atom at the halogen atom in halomethanes is expected to be extremely favourable, especially at bromine and iodine and that intermediates are not likely to be involved in the reaction mechanism.

Reaction of Methyl Radical with Halomethanes

The hypervalent dimethyl λ^3 -halogenyl species (8), which include dimethyl- λ^3 -chlorinyl (Me₂Cl), dimethyl- λ^3 -brominyl (Me₂Br) and dimethyl- λ^3 -iodinyl (Me₂I) were located on their respective potential energy surfaces. Structures (8) are predicted to have colinear arrangements of attacking and leaving groups in all cases and to correspond to transition states at both SCF and MP2 levels of theory. Calculated geometries are

displayed in Figure 3, while the energy barriers (ΔE^\ddagger) for the reactions as depicted in Scheme 4 are listed in Table 2. Calculated energies of the structures (8) are also listed in Table 5.

Scheme 4

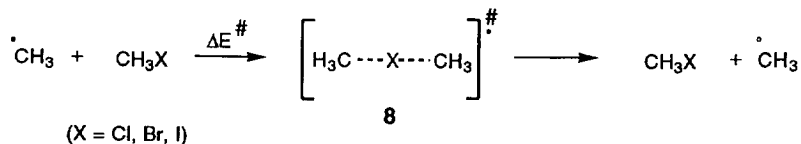


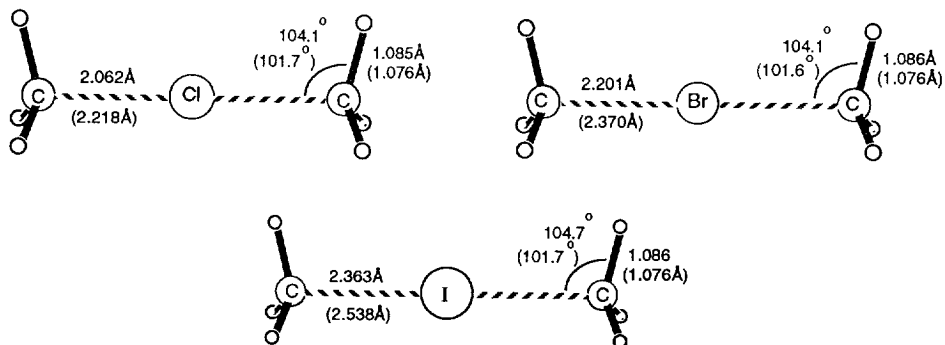
Table 3. SCF, MP2 and QCISD/MP2 Calculated Energy Barriers^a (ΔE^\ddagger) for the Homolytic Substitution Reactions of Methyl Radical at the Halogen in Chloromethane, Bromomethane and Iodomethane (Scheme 4).

Transition State (8)	SCF	MP2	QCISD/MP2
	ΔE^\ddagger	ΔE^\ddagger	ΔE^\ddagger
Me ₂ Cl	141.1	127.9	117.6
Me ₂ Br	99.7	93.4	81.9
Me ₂ I	68.0	65.0	53.2

^aEnergies in kJ.mol⁻¹. For details of the basis set used, see text.

The transition states (8) depicted in Figure 3 are *later* than those for the attack of methyl radical at hydrogen halides depicted in Figure 2 (reverse reaction in Scheme 3) with MP2-calculated C-X distances of 2.063Å (Cl), 2.201Å (Br) and 2.363Å (I), reflecting the greater leaving group ability of methyl radical over hydrogen atom, as expected.

Figure 3. MP2 Calculated Geometries^a of the Transition States (8) involved in the Homolytic Substitution of Methyl Radical at the Halogen in Chloromethane, Bromomethane and Iodomethane (MP2 Data in Parentheses).



^aFor description of basis set used, see text.

The reactions depicted in Scheme 4 are representative of *halogen transfer* reactions and their synthetic utility has been highlighted by Curran and coworkers.^{1,29} The calculations reported in this work provide mechanistic insight into these reactions; halogen transfer between carbon centres prefers a colinear arrangement of attacking and leaving radicals and that iodine is predicted to undergo transfer most efficiently.

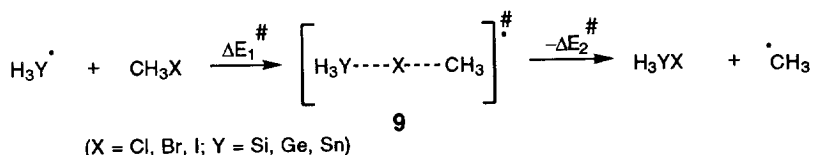
It is interesting to compare these calculated data to those for the analogous homolytic substitution by methyl radical at the sulfur atom in methanethiol, the selenium atom in methaneselenol and the tellurium atom in methanetellurol performed at the same level of theory.¹⁹ These reactions are predicted to involve energy barriers of 89.1 kJ.mol⁻¹, 63.0 kJ.mol⁻¹, and 29.7 kJ.mol⁻¹ respectively with the formation of a short-lived hypervalent (dimethyl-λ⁴-telluryl) intermediate in the reaction involving tellurium.

The following order of reactivity for homolytic substitution by methyl radical is therefore suggested: Cl < S < Br < Se < I < Te and is in qualitative agreement with available rate data for the attack of a variety of carbon-centred radicals at these heteroatoms.^{30,31}

Reaction of Silyl, Germyl and Stannyl Radical with Halomethanes

As discussed previously, free radical halogen abstraction by silicon-, germanium- and tin- centred chain-carrying radicals is a convenient and popular method for the generation of carbon-centred radicals despite the mechanistic details of the reaction not having been adequately resolved.

Scheme 5



We therefore modelled the abstraction of halogen from chloro-, bromo- and iodomethane by silyl ($\bullet\text{SiH}_3$), germyl ($\bullet\text{GeH}_3$) and stannyl ($\bullet\text{SnH}_3$), radicals (Scheme 5). At both SCF and MP2 levels of theory, only colinear transition states (**9**) could be located on the appropriate potential energy surfaces, strongly suggesting that these chain-carrying radicals also abstract halogen from alkyl halides via smooth transition states. Of particular interest is abstraction of iodine which, has been speculated previously^{20,21} to involve hypervalent iodanyl radical intermediates. Calculated transition states (**9**) are displayed in Figure 4, calculated energy barriers (ΔE_1^\ddagger , ΔE_2^\ddagger) for the forward and reverse reactions are listed in Table 4, while calculated energies of **9** are listed in Table 5.

Inspection of Table 4 reveals some interesting features. For each abstracting radical, iodine is the easiest of the halogens to abstract, while chlorine is the most difficult. QCISD/MP2 Calculated energy barriers range from 80.3 kJ.mol⁻¹ for the abstraction of chlorine by stannyl to 21.8 kJ.mol⁻¹ for the abstraction of iodine by silyl.

On the other hand, silyl appears to be a better halogen abstractor than germyl which, in turn, is marginally better than stannyl. QCISD/MP2 Calculated energy barriers range from 21.8 kJ.mol⁻¹ for the abstraction of iodine by silyl to 24.7 kJ.mol⁻¹ for the abstraction of iodine by germyl and 27.2 for the abstraction of iodine by stannyl. All reactions are predicted to be substantially exothermic. These low barriers and exothermicities are undoubtedly responsible for the success which these reagents have had in the generation of alkyl radicals for synthetic and other purposes. The reverse reactions also display some interesting trends, with the stannyl and germyl radicals being substantially better leaving groups than silyl; QCISD/MP2 calculated barriers for the reverse reaction at iodine range from 86.6 kJ.mol⁻¹ (silyl) to 69.4 kJ.mol⁻¹ (germyl) and 65.2 kJ.mol⁻¹ (stannyl).

Table 4. SCF, MP2 and QCISD/MP2 Calculated Energy Barriers^a (ΔE_1^\ddagger , ΔE_2^\ddagger) for the Forward and Reverse Homolytic Substitution Reactions of Silyl ($\cdot\text{SiH}_3$), Germyl ($\cdot\text{GeH}_3$) and Stannyl ($\cdot\text{SnH}_3$) Radicals at the Halogen Atom in Chloromethane, Bromomethane and Iodomethane (Scheme 5).

Transition State (9)	SCF		MP2		QCISD/MP2	
	ΔE_1^\ddagger	ΔE_2^\ddagger	ΔE_1^\ddagger	ΔE_2^\ddagger	ΔE_1^\ddagger	ΔE_2^\ddagger
H ₃ SiClCH ₃	95.8	211.8	98.2	183.2	73.7	160.7
H ₃ GeClCH ₃	98.1	179.1	85.7	133.3	78.8	128.8
H ₃ SnClCH ₃	96.2	167.0	87.5	119.4	80.3	114.9
H ₃ SiBrCH ₃	61.6	168.5	52.0	126.1	44.3	121.3
H ₃ GeBrCH ₃	63.2	144.7	56.6	102.3	48.3	97.3
H ₃ SnBrCH ₃	62.1	138.8	59.2	94.7	50.4	89.4
H ₃ SiICH ₃	36.7	130.2	30.3	91.2	21.8	86.6
H ₃ GeICH ₃	37.6	114.1	33.6	74.3	24.7	69.4
H ₃ SnICH ₃	37.2	112.2	36.7	70.5	27.2	65.2

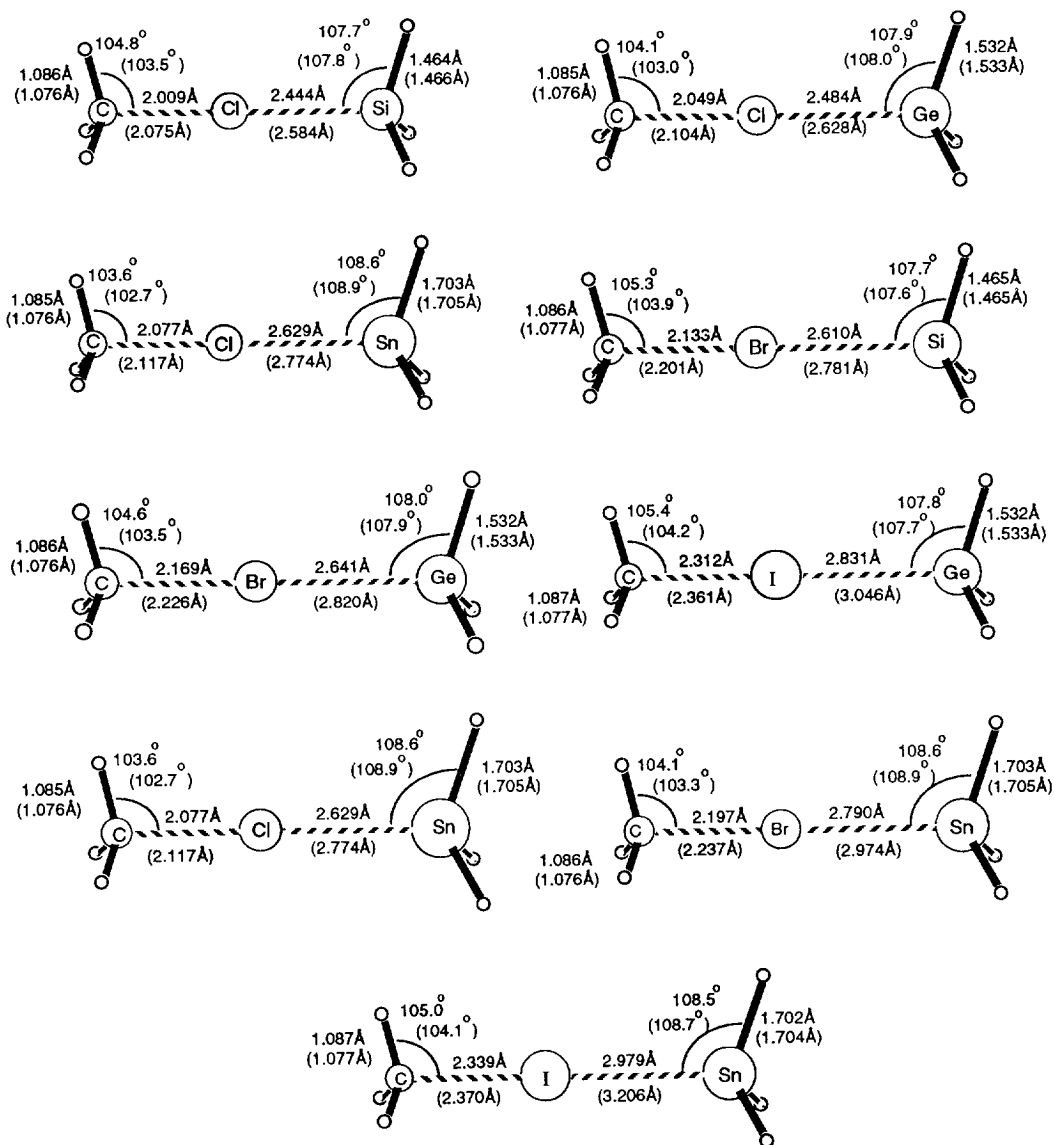
^aEnergies in kJ.mol⁻¹. For details of the basis set used, see text.

It is interesting to compare these data with those for the analogous homolytic reactions at the selenium atom in alkyl selenides and the tellurium atom in alkyl tellurides which are also predicted to proceed via smooth transition states in all cases.^{18,32} MP4/HUZ-SV**//HF/HUZ-SV** Calculations predict an energy barrier of only 12.6 kJ.mol⁻¹ for attack of silyl radical at the selenium atom in methaneselenol, while QCISD/MP2 calculations using the more flexible double- ζ pseudopotential basis sets of Hay and Wadt³² predict barriers of 35.5, 44.3 and 59.2 kJ.mol⁻¹ for attack of silyl, germyl and stannyl radical respectively at methaneselenol, and barriers of 9.6, 19.9 and 30.1 kJ.mol⁻¹ for the analogous reactions respectively at methanetellurol.³² Clearly then, silyl radical is predicted to be more selective toward chalcogen than halogen (9.6 (Si/Te) vs. 21.8 kJ.mol⁻¹ (Si/I); 35.5 (Si/Se) vs. 44.3 kJ.mol⁻¹ (Si/Br)) when compared with germyl or stannyl which are predicted to be less selective toward chalcogen over halogen than the silicon analogue (19.9 (Ge/Te) vs. 24.7 kJ.mol⁻¹ (Ge/I); 44.3 (Ge/Se) vs. 48.3 kJ.mol⁻¹ (Ge/Br); 30.1 (Sn/Te) vs. 27.2 kJ.mol⁻¹ (Sn/I); 52.9 (Sn/Se) vs. 50.4 kJ.mol⁻¹ (Sn/Br) vs.). Indeed, stannyl radical is predicted to have a slight preference for attack at halogen over chalcogen.

Unfortunately, little experimental data are available to allow meaningful comparisons to be made, especially in reactions involving tellurium. Available data include rate constants of 8.1×10^9 and 2.5×10^9 M⁻¹s⁻¹ for attack of triethylsilyl and tri-*n*-butylstannyl radicals respectively at iodomethane in solution at 300K,¹² a factor of 3.2 in favour of the triethylsilyl radical. This is in good agreement with our gas-phase prediction of a factor of approximately 8 on the basis of our calculated activation barriers for silyl and stannyl radical attack at iodomethane, assuming similar entropy terms. In addition attack of tris(trimethylsilyl)silyl radicals at primary phenylselenide and bromide have associated rate constants of 9.6×10^7 and 4.6×10^7 M⁻¹s⁻¹ respectively at 25°,¹⁴ while tri-*n*-butylstannyl radicals are approximately 10 times more selective (at 25°) for bromine (over phenylselenide) than are tri-*n*-butylgermyl radicals.^{9,10} For example tri-*n*-butylgermyl radical reacts with 1-bromoheptane and 3-phenylselenotetrahydrofuran with rate constants of 4.6×10^7 and 1.6×10^7

$M^{-1}s^{-1}$,¹⁰ while rate constants for the similar reactions using tri-*n*-butylstannyl radicals have been determined to be 2.6×10^7 and 6.6×10^5 respectively.⁹ These data in excellent agreement with our prediction of a factor of approximately 14 based on our calculated data, assuming similar entropic factors.

Figure 4. MP2 Calculated Geometries^a of the Transition States (8) involved in the Homolytic Substitution of Silyl (SiH₃), Germeryl (GeH₃) and Stannyl (SnH₃) Radical at the Halogen in Chloromethane, Bromomethane and Iodomethane (MP2 Data in Parentheses).



^aFor description of basis set used, see text.

Table 5. SCF, MP2 and QCISD/MP2 Calculated Energies^a of the Reactants, Products and Transition States (7, 8, 9) in this Study.

Structure	SCF	MP2	QCISD/MP2
·H	-0.49764	-	-
·CH ₃	-39.57191	-39.69802	-39.71956
·SiH ₃	-5.46984	-5.55964	-5.58357
·GeH ₃	-5.34597	-5.43346	-5.45694
·SnH ₃	-4.94363	-5.02396	-5.04697
HCl	-15.30589	-15.44716	-15.46199
HBr	-13.52138	-13.64640	-13.66109
HI	-11.74291	-11.85297	-11.86688
CH ₃ Cl	-54.34201	-54.62010	-54.64971
CH ₃ Br	-52.56025	-52.82449	-52.85200
CH ₃ I	-50.78407	-51.03446	-51.06044
H ₃ SiCl	-20.28419	-20.51412	-20.54686
H ₃ SiBr	-18.49889	-18.71432	-18.74536
H ₃ SiI	-16.71761	-16.91927	-16.94911
H ₃ GeCl	-20.14693	-20.37368	-20.40610
H ₃ GeBr	-18.36535	-18.57735	-18.60804
H ₃ GeI	-16.58725	-16.78540	-16.81481
H ₃ SnCl	-19.74069	-19.95821	-19.99031
H ₃ SnBr	-17.96107	-18.16394	-18.19430
H ₃ SnI	-16.18436	-16.37328	-16.40230
CH ₃ ClH	-54.80253	-55.08253	-55.11966
CH ₃ BrH	-53.03412	-53.29719	-53.33288
CH ₃ IH	-51.26711	-51.51474	-51.54916
Me ₂ Cl	-93.86019	-94.26940	-94.32449
Me ₂ Br	-92.09420	-92.48695	-92.54036
Me ₂ I	-90.33009	-90.70775	-90.75976
H ₃ SiClCH ₃	-59.77535	-60.14236	-60.20522
H ₃ GeClCH ₃	-59.65063	-60.02092	-60.07662
H ₃ SnClCH ₃	-59.24901	-59.61075	-59.66612
H ₃ SiBrCH ₃	-58.00663	-58.36430	-58.41870
H ₃ GeBrCH ₃	-57.88216	-58.23641	-58.29054
H ₃ SnBrCH ₃	-57.48022	-57.82591	-57.87980
H ₃ SiI ₂ CH ₃	-56.23992	-56.58258	-56.63570
H ₃ GeI ₂ CH ₃	-56.11573	-56.45511	-56.50795
H ₃ SnI ₂ CH ₃	-55.71352	-56.04444	-56.09704

Conclusions

High-level *ab initio* calculations predict that homolytic substitutions by hydrogen atom, methyl, silyl, germyl and stannyl radicals proceed via mechanisms which do not involve hypervalent 9-X-3 intermediates. Apart from reactions involving hydrogen atom, these processes adopt co-linear arrangements of attacking and leaving radicals with, as expected, substitution at iodine being more facile than the analogous reaction at bromine, which in turn is more reactive than chlorine. Silicon-centred radicals are predicted to be more selective toward chalcogen abstraction over the halogen of the same row of the periodic table than germanium-centred radicals, which, in turn are more selective than tin-centred radicals.

We thank the Australian Research Council for financial support.

References and Notes

1. Giese, B., *Radicals in Organic Synthesis: Formation of Carbon-Carbon Bonds*, 1986, Pergamon Press, Oxford; and references cited therein.
2. Julia, M. *Pure Appl. Chem.*, 1974, 40, 553; Julia, M., Maumy, M. *Bull. Soc. Chim. Fr.*, 1968, 1603; Julia, M., Descoins, C., Baillarge, M., Jacquet, B., Uguen, D., Groeger, F.A., *Tetrahedron*, 1975, 37, 1737.
3. Griller, D., Ingold, K. U. *Acc. Chem. Res.*, 1980, 13, 317 and refs. cited therein.
4. Beckwith, A. L. J., Ingold, K. U., *Rearrangements in Ground and Excited States*, de Mayo, P. Ed., Academic Press: New York, 1980.
5. Beckwith, A. L. J., *Tetrahedron*, 1981, 37, 3073 and refs. cited therein; Beckwith, A. L. J., Schiesser, C. H., *Tetrahedron*, 1985, 41, 3925.
6. Tedder, J. M.; Walton, J. C., *Acc. Chem. Res.*, 1976, 9, 183. Tedder, J. M.; Walton, J. C., *Tetrahedron*, 1980, 36, 701. Ruechardt, C., *Topics in Current Chem.*, 1980, 88, 1. Wilt, J. W., *Free Radicals*, (Kochi, J. K. ed.), 1973, Vol. 1., 333, Wiley, New York. Surzur, J. -M. in *Reactive Intermediates*, (Abramovitch, A. A. ed.), 1981, Vol. 2, Chap. 3., Plenum Press, New York.
7. Barton, D. H. R., *Tetrahedron*, 1992, 48, 2529; and refs. cited therein.
8. Neumann, W. P., *Synthesis*, 1987, 665; Curran, D. P., *Synthesis*, 1988, 417; Curran, D. P., *Synthesis*, 1988, 489; Curran, D. P., Jasperese, C. P., Totleben, M. J., *J. Org. Chem.*, 1991, 56, 7169.
9. Beckwith, A. L. J., Pigou, P. E., *Aust. J. Chem.*, 1986, 39, 77.
10. Beckwith, A. L. J., Pigou, P. E., *Aust. J. Chem.*, 1986, 39, 1151.
11. Beckwith, A. L. J., Roberts, D. H., Schiesser, C. H., Wallner, A., *Tetrahedron Lett.*, 1985, 26, 3349.
12. Chatgialiloglu, C., Ingold, K. U., Scaiano, J. C., *J. Am. Chem. Soc.*, 1982, 104, 5123
13. Luszytk, J, Maillard, B., Ingold, K. U., *J. Org. Chem.*, 1986, 51, 2457.

14. Ballestri, M., Chatgililoglu, C., Clark, K. B., Griller, D., Giese, B., Kopping, B., *J. Org. Chem.*, **1991**, *56*, 678.
15. Smart, B. A., Schiesser, C. H., *J. Comput. Chem.*, (in press).
16. Lyons, J. E., Schiesser, C. H., *J. Chem. Soc. Perkin Trans. 2*, **1992**, 1655.
17. Ferris, K. F., Franz, J. A., *J. Org. Chem.*, **1992**, *57*, 777.
18. Schiesser, C. H., Sutej, K., *J. Chem. Soc. Chem. Commun.*, **1992**, 57; Lyons, J. E., Schiesser, C. H., *J. Organometal. Chem.*, **1992**, *437*, 165.
19. Smart, B. A., Schiesser, C. H., *J. Chem. Soc. Perkin Trans. 2*, **1994**, 2269.
20. Minisci, F., Fontana, F., Pianese, G., Yan, Y. M., *J. Org. Chem.*, **1993**, *58*, 4207; Minisci, F., Coppa, F., Fontana, F., Pianese, G., Zhao, L., *J. Org. Chem.*, **1992**, *57*, 3929.
21. Minisci, F. in *Sulfur-Centered Reactive Intermediates in Chemistry and Biology*; Chatgililoglu, C., Asmus, K. D. Eds., Plenum Press: New York, **1990**.
22. Frisch, M. J., Trucks, G. W., Head-Gordon, M., Gill, P. M. W., Wong, M. W., Foresman, J. B., Johnson, B. G., Schlegel, H. B., Robb, M. A., Replogle, E.S., Gomperts, R., Andres, J. L., Raghavachari, K., Binkley, J. S., Gonzales, C., Martin, R.L., Fox, D. J., Defrees, D. J., Baker, J., Stewart, J. J. P., Pople, J. A. **1992**, *Gaussian 92*, Revision F, Gaussian Inc, Pittsburgh, PA. All calculations were performed on either a Sun Sparcserver 10/512 or Cray Y-MP4E/364
23. Values of $\langle S^2 \rangle$ never exceeded 0.87 before annihilation of quartet contamination indicating the presence of only moderate spin contamination.
24. Wadt, W. R., Hay, P. J., *J. Chem. Phys.*, **1985**, *82*, 284.
25. Hay, P. J., Wadt, W. R., *J. Chem. Phys.*, **1985**, *82*, 270.
26. Hay, P. J., Wadt, W. R., *J. Chem. Phys.*, **1985**, *82*, 299.
27. Höllwarth, A., Böhme, M., Dapprich, S., Ehlers, A. W., Gobbi, A., Jonas, V., Köhler, K. F., Stegmann, R., Veldkamp, A., Frenking, G., *Chem. Phys. Lett.*, **1993**, *208*, 237.
28. Dunning, T. H., Hay, P. J., *Modern Theoretical Chemistry*, **1976**, Plenum, New York, pp. 1-28 ch. 1.
29. Curran, D. P., Chang, C.-T., *J. Org. Chem.*, **1989**, *54*, 3140; Curran, D. P., Bosch, E., Kaplan, J., Newcomb, M., *J. Org. Chem.*, **1989**, *54*, 1826; Curran, D. P., Chen, M.-H., Kim, D., *J. Am. Chem. Soc.*, **1989**, *111*, 6265; Curran, D. P., Kim, D., *Tetrahedron*, **1991**, *47*, 6171; Curran, D. P., Kim, D., Ziegler, C., *Tetrahedron*, **1991**, *47*, 6189; Curran, D. P., Seong, C. M., *Tetrahedron*, **1992**, *48*, 2175.
30. Newcomb, M., Sanchez, R. M., Kaplan, J., *J. Am. Chem. Soc.*, **1987**, *109*, 1195.
31. Curran, D. P., Martin-Esker, A. A., Ko, S.-B., Newcomb, M., *J. Org. Chem.*, **1993**, *58*, 4691.
32. Schiesser, C. H., Smart, B. A., manuscript in preparation.

(Received in UK 30 December 1994; accepted 13 January 1995)